

Effective wave equations for the dynamics of cigar-shaped and disk-shaped Bose condensates

L. Salasnich,¹ A. Parola,² and L. Reatto¹¹*Istituto Nazionale per la Fisica della Materia, Unità di Milano Università, Dipartimento di Fisica, Università di Milano, Via Celoria 16, 20133 Milano, Italy*²*Istituto Nazionale per la Fisica della Materia, Unità di Como, Dipartimento di Scienze Fisiche, Università dell'Insubria, Via Valleggio 11, 23100 Como, Italy*

(Received 1 June 2001; revised manuscript received 25 September 2001; published 2 April 2002)

Starting from the three-dimensional (3D) Gross-Pitaevskii equation and using a variational approach, we derive an effective 1D wave equation that describes the axial dynamics of a Bose condensate confined in an external potential with cylindrical symmetry. The trapping potential is harmonic in the transverse direction and generic in the axial one. Our equation, that is a time-dependent nonpolynomial nonlinear Schrödinger equation (1D NPSE), can be used to model cigar-shaped condensates, whose dynamics is essentially 1D. We show that 1D NPSE gives much more accurate results than all other effective equations recently proposed. By using 1D NPSE we find analytical solutions for bright and dark solitons, which generalize the ones known in the literature. We deduce also an effective 2D nonpolynomial Schrödinger equation (2D NPSE) that models disk-shaped Bose condensates confined in an external trap that is harmonic along the axial direction and generic in the transverse direction. In the limiting cases of weak and strong interaction, our approach gives rise to Schrödinger-like equations with different polynomial nonlinearities.

DOI: 10.1103/PhysRevA.65.043614

PACS number(s): 03.75.Fi, 51.10.+y

I. INTRODUCTION

Bose condensates are nowadays routinely produced by many experimental groups all over the world. The thermal and dynamical properties of Bose condensates have been investigated with different atomic species and various trap geometries. An interesting theoretical problem is the derivation of one dimensional (1D) and 2D equations, describing cigar-shaped and disk-shaped condensates, respectively. At zero temperature, a good theoretical tool for the study of the dynamics of dilute condensates is the time-dependent 3D Gross-Pitaevskii equation [1]. In the case of reduced dimensionality, various approaches have been adopted to derive effective equations from the 3D Gross-Pitaevskii equation [2–4].

In this paper we analyze both cigar-shaped and disk-shaped condensates. By using a variational approach, we obtain an effective 1D time-dependent nonpolynomial nonlinear Schrödinger equation that describes the axial dynamics of a Bose condensate confined in an external potential with cylindrical symmetry. We demonstrate that our equation exactly reproduces previous findings in the limits of weak coupling and strong coupling. Moreover, we show that our variational approach is more accurate than all other recently proposed procedures in the evaluation of both static and dynamical properties of the condensate. We also investigate the 2D reduction of the 3D Gross-Pitaevskii equation. In this case it is not possible to analytically determine a single effective 2D wave equation which describes the dynamics of disk-shaped condensates. Nevertheless, analytical equations can be found in the weakly interacting limit and in the strongly interacting limit.

II. EFFECTIVE 1D EQUATION

The 3D Gross-Pitaevskii equation (3D GPE), which describes the macroscopic wave function $\psi(\mathbf{r},t)$ of the Bose condensate, is given by

$$i\hbar \frac{\partial}{\partial t} \psi(\mathbf{r},t) = \left[-\frac{\hbar^2}{2m} \nabla^2 + U(\mathbf{r}) + gN|\psi(\mathbf{r},t)|^2 \right] \psi(\mathbf{r},t), \quad (1)$$

where $U(\mathbf{r})$ is the external trapping potential and $g = 4\pi\hbar^2 a_s/m$ is the scattering amplitude and a_s the s -wave scattering length [1]. N is the number of condensed bosons and the wave function is normalized to one. Note that the 3D GPE is accurate to describe a condensate of dilute bosons only near zero temperature, where thermal excitations can be neglected [5].

The 3D GPE can be obtained by using the quantum least action principle, i.e., 3D GPE is the Euler-Lagrange equation of the following action functional:

$$S = \int dt d\mathbf{r} \psi^*(\mathbf{r},t) \left[i\hbar \frac{\partial}{\partial t} + \frac{\hbar^2}{2m} \nabla^2 - U(\mathbf{r}) - \frac{1}{2} gN|\psi(\mathbf{r},t)|^2 \right] \psi(\mathbf{r},t). \quad (2)$$

We consider an external potential with cylindrical symmetry. In particular we analyze a trapping potential that is harmonic in the transverse direction and generic in the axial direction: $U(\mathbf{r}) = \frac{1}{2} m\omega_{\perp}^2(x^2 + y^2) + V(z)$. We want to minimize the action functional S by choosing an appropriate trial wave function. A natural choice [3] is the following:

$$\psi(\mathbf{r},t) = \phi(x,y,t; \sigma(z,t)) f(z,t), \quad (3)$$

where both ϕ and f are normalized and ϕ is represented by a Gaussian

$$\phi(x,y,t; \sigma(z,t)) = \frac{e^{[-(x^2+y^2)]/2\sigma(z,t)^2}}{\pi^{1/2}\sigma(z,t)}. \quad (4)$$

The variational functions $\sigma(z,t)$ and $f(z,t)$ will be determined by minimizing the action functional after integration in the (x,y) plane. The choice of a Gaussian shape for the condensate in the transverse direction is well justified in the limit of weak interatomic coupling, because the exact ground state of the linear Schrödinger equation with harmonic potential is a Gaussian. Moreover, for the description of the collective dynamics of Bose-Einstein condensates, it has already been shown that the variational technique based on Gaussian trial functions leads to reliable results even in the large condensate number limit [6,7].

We assume that the transverse wave-function ϕ is slowly varying along the axial direction with respect to the transverse direction [3], i.e., $\nabla^2\phi \approx \nabla_{\perp}^2\phi$ where $\nabla_{\perp}^2 = \partial^2/\partial x^2 + \partial^2/\partial y^2$. By inserting the trial wave function in Eq. (2) and after spatial integration along x and y variables the action functional becomes

$$S = \int dt dz f^* \left[i\hbar \frac{\partial}{\partial t} + \frac{\hbar^2}{2m} \frac{\partial^2}{\partial z^2} - V - \frac{1}{2} g N \frac{\sigma^{-2}}{2\pi} |f|^2 - \frac{\hbar^2}{2m} \sigma^{-2} - \frac{m\omega_{\perp}^2}{2} \sigma^2 \right] f. \quad (5)$$

The Euler-Lagrange equations with respect to f^* and σ read

$$i\hbar \frac{\partial}{\partial t} f = \left[-\frac{\hbar^2}{2m} \frac{\partial^2}{\partial z^2} + V + g N \frac{\sigma^{-2}}{2\pi} |f|^2 + \left(\frac{\hbar^2}{2m} \sigma^{-2} + \frac{m\omega_{\perp}^2}{2} \sigma^2 \right) \right] f, \quad (6)$$

$$\frac{\hbar^2}{2m} \sigma^{-3} - \frac{1}{2} m \omega_{\perp}^2 \sigma + \frac{1}{2} g N \frac{\sigma^{-3}}{2\pi} |f|^2 = 0. \quad (7)$$

The second Euler-Lagrange equation reduces to an algebraic relation providing a one-to-one correspondence between σ and f : $\sigma^2 = a_{\perp}^2 \sqrt{1 + 2a_s N |f|^2}$, where $a_{\perp} = \sqrt{\hbar/m\omega_{\perp}}$ is the oscillator length in the transverse direction. One sees that σ depends implicitly on z and t because of the space and time dependence of $|f|^2$. Inserting this result in the first equation one finally obtains

$$i\hbar \frac{\partial}{\partial t} f = \left[-\frac{\hbar^2}{2m} \frac{\partial^2}{\partial z^2} + V + \frac{gN}{2\pi a_{\perp}^2} \frac{|f|^2}{\sqrt{1 + 2a_s N |f|^2}} + \frac{\hbar\omega_{\perp}}{2} \left(\frac{1}{\sqrt{1 + 2a_s N |f|^2}} + \sqrt{1 + 2a_s N |f|^2} \right) \right] f. \quad (8)$$

This equation is the main result of our paper. It is a time-dependent nonpolynomial nonlinear Schrödinger equation (1D NPSE).

We observe that from 1D NPSE in certain limiting cases one recovers familiar results. In the weakly interacting limit $a_s N |f|^2 \ll 1$ one has $\sigma^2 = a_{\perp}^2$ and the previous equation reduces to

$$i\hbar \frac{\partial}{\partial t} f = \left[-\frac{\hbar^2}{2m} \frac{\partial^2}{\partial z^2} + V + \frac{gN}{2\pi a_{\perp}^2} |f|^2 \right] f, \quad (9)$$

where the additive constant $\hbar\omega_{\perp}$ has been omitted because it does not affect the dynamics. This equation is a 1D Gross-Pitaevskii equation. The nonlinear coefficient g' of this 1D GPE can be thus obtained from the nonlinear coefficient g of the 3D GPE by setting $g' = g/(2\pi a_{\perp}^2)$. This ansatz has been already used by various authors, for example in Ref. [2]. Note that the limit $a_s N |f|^2 \ll 1$ is precisely the regime where the healing length is larger than σ . In this regime the cigar-shaped condensate is quasi-1D, as shown in a recent experiment [8]. It is well known that in 1D and at ultra-low densities ($a_s N |f|^2 \ll a_s^2/a_{\perp}^2 \ll 1$) an interacting Bose gas becomes a Tonks gas, i.e., a gas of spinless Fermions [9]. Such a transition cannot be described by the cubic 3D GPE equation and therefore by 1D NPSE because in the Tonks regime the interatomic interaction cannot simply be approximated by a zero-range pseudopotential in mean-field approximation [10]. Instead, in the strongly interacting high-density limit $a_s N |f|^2 \gg 1$ (but $N|\psi|^2 a_s \ll 1$ to satisfy the diluteness condition) one finds $\sigma^2 = \sqrt{2} a_{\perp}^2 a_s^{1/2} N^{1/2} |f|$ and the 1D NPSE becomes

$$i\hbar \frac{\partial}{\partial t} f = \left[-\frac{\hbar^2}{2m} \frac{\partial^2}{\partial z^2} + V + \frac{3}{2} \frac{gN^{1/2}}{2\pi a_{\perp}^2 \sqrt{2} a_s} |f| \right] f. \quad (10)$$

In this limit, and in the stationary case, the kinetic term can be neglected (Thomas-Fermi approximation) and one finds the following analytical formula for the axial density profile:

$$|f(z)|^2 = \frac{2}{9} \frac{1}{(\hbar\omega_{\perp})^2 a_s N} [\mu' - V(z)]^2, \quad (11)$$

where μ' is the chemical potential, fixed by the normalization condition. It is important to stress that this 1D Thomas-Fermi density profile is quadratic in the term $\mu' - V(z)$. The same quadratic dependence is obtained starting from the Thomas-Fermi approximation of the 3D stationary GPE, i.e., neglecting the spatial derivatives in Eq. (1), and then integrating along x and y variables. In this way one finds a formula that differs from Eq. (11) only for the numerical factor which is 1/4 instead of 2/9.

To test the accuracy of the full 1D NPSE, Eq. (8), and compare it with other procedures proposed in the last few years, we numerically investigate the simple case of harmonic trapping also in the axial direction: $V(z) = \frac{1}{2} m \omega_z^2 z^2$. In this case, the 1D NPSE can be written in scaled units: z in units of $a_z = \sqrt{\hbar/m\omega_z}$, the oscillator length in the axial direction, and t in units of $1/\omega_z$. In order to assess the accuracy of the various 1D approximations we have also solved numerically the 3D Gross-Pitaevskii equation (3D GPE), given by Eq. (1) with imaginary time [11]. Note that the numerical solution of the 1D NPSE is not more time consuming than the solution of the standard 1D GPE. In Fig. 1 we plot the normalized density profile $\rho(z) = |f(z)|^2$ of the ground-state

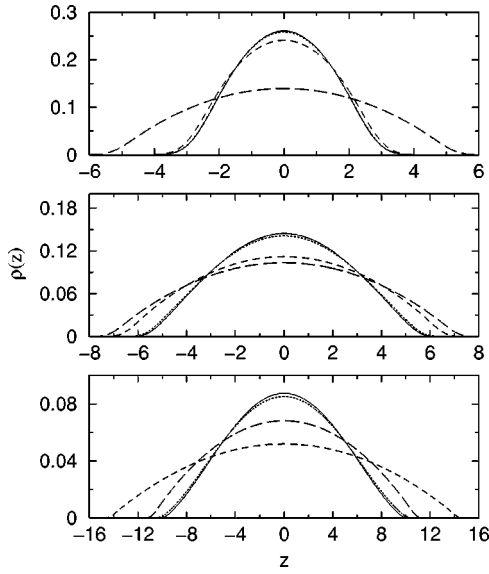


FIG. 1. Normalized density profile $\rho(z) = |f(z)|^2$ along the axial direction z for the cigar-shaped trap. Number of Bosons: $N = 10^4$ and trap anisotropy: $\omega_{\perp}/\omega_z = 10$. Four different procedures: 3D GPE (solid line), 1D GPE (dashed line), CGPE (long-dashed line), and 1D NPSE (dotted line). From top to bottom: $a_s/a_z = 10^{-4}$, $a_s/a_z = 10^{-3}$, and $a_s/a_z = 10^{-2}$. Length z in units of a_z and density in units of a_z^{-1} .

wave function of a cigar-shaped condensate confined in a trap with an aspect ratio $a_z/a_{\perp} = 10$.

We compare the results of four different procedures. The first procedure is the “exact” one, i.e., the solution of the 3D GPE. The second procedure is the numerical solution of the 1D Gross-Pitaevskii equation (1D GPE) given by Eq. (9) with an imaginary time. The third procedure is that proposed by Chiofalo and Tosi [4]. In this case the nonlinear term of the 1D Gross-Pitaevskii equation is found by imposing that the 1D wave function has the same chemical potential of the 3D one (CGPE). The fourth and last procedure is the numerical solution of our nonpolynomial nonlinear Schrödinger equation (1D NPSE), i.e., Eq. (8) with imaginary time. As shown in Fig. 1, the 1D NPSE results are always very close to the “exact” ones and much better than the other approximations. Moreover, the CGPE procedure gives better results than the 1D GPE for large values of the scattering length where Eq. (9) is not reliable but in any case the 1D NPSE is superior.

The very good performance of Eq. (8) is not limited to the ground state. We have investigated the dynamics of the condensate by taking the previously calculated ground-state wave functions but changing the harmonic trap in the axial direction: from $V(z) = \frac{1}{2}m\omega_z^2 z^2$ to $V(z) = \frac{2}{5}m\omega_z^2 z^2$. In this way the condensate shows large collective shape oscillations along the z axis.

In Fig. 2 we plot the time evolution of the squared amplitude $\langle z^2 \rangle$ of the condensate in the axial direction, given by $\langle z^2 \rangle = \int dz z^2 \rho(z, t)$, where $\rho(z, t) = \int dx dy |\psi(\mathbf{r}, t)|^2$ in the case of the 3D GPE and $\rho(z, t) = |f(z, t)|^2$ in the other cases. Apart the better evaluation of the amplitude that is a consequence of the better evaluation of the ground-state wave

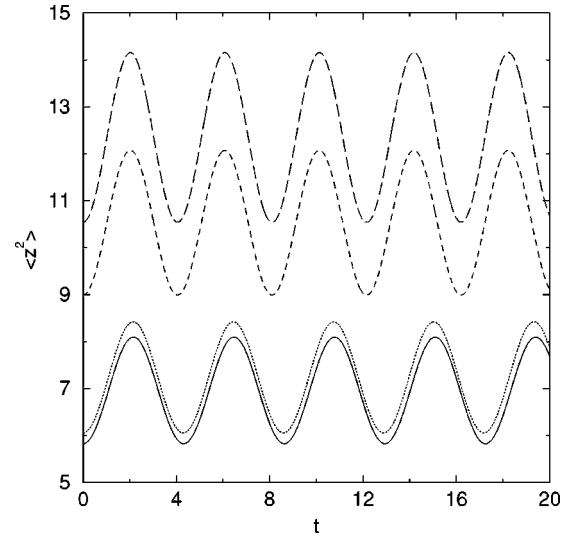


FIG. 2. Squared amplitude $\langle z^2 \rangle$ as a function of time t . Number of Bosons: $N = 10^4$ and trap anisotropy: $\omega_{\perp}/\omega_z = 10$. Four different procedures: 3D GPE (solid line), 1D GPE (dashed line), CGPE (long-dashed line), and 1D NPSE (dotted line). Scattering length: $a_s/a_z = 10^{-3}$. Length z in units of a_z , density in units of a_z^{-1} , and time t in units of $1/\omega_z$.

function, one sees that our 1D NPSE reproduces quite well also the “exact” sinusoidal behavior of the collective oscillation. For example, after four oscillations the relative error in the determination of the instant t of minimum radius $\langle z^2 \rangle$ is about 1%. The other two procedures (CGPE and 1D GPE) clearly show a frequency delay with respect to the 3D GPE and 1D NPSE results: after four oscillations their relative errors, with respect to the 3D GPE result, are about 5 and 6% respectively.

We remind that the 1D NPSE has been obtained by using a factorization of the 3D wave function with a variational ansatz for the transverse part of the wave function and neglecting the term $\hbar^2/2m\phi^* \partial^2 \phi / \partial z^2$. Under the condition of the present computations the last assumption is fully justified because we have numerically verified that the ratio between the neglected term and the total energy ranges from 10^{-3} in the weak-coupling limit to 10^{-7} in the strong-coupling limit.

To test the accuracy of 1D NPSE in the description of the dynamics of a cigar-shaped Bose condensate in a more complex problem, we investigate the scattering and tunneling of the condensate on a Gaussian barrier. The initial wave function of the condensate is found by solving the equations with imaginary time and imposing a harmonic trapping potential also in the horizontal axial direction

$$V(z) = \frac{1}{2}m\omega_z^2(z - z_0)^2. \quad (12)$$

To have a cigar-shaped condensate we choose $\omega_{\perp}/\omega_z = 10$. We set $z_0 = 20$, where z_0 is written in units of the harmonic length $a_z = (\hbar/m\omega_z)^{1/2}$. For $t > 0$ the trap in the axial direction is switched off and a Gaussian energy barrier is inserted at $z = 0$. The potential barrier is given by

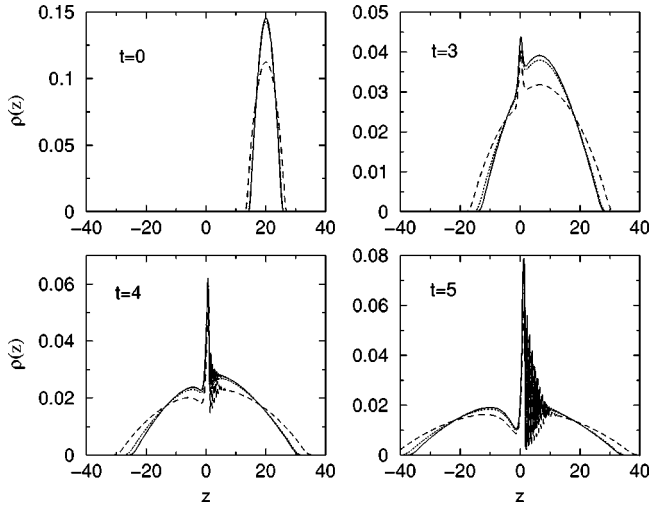


FIG. 3. Four frames of the axial density profile $\rho(z)$ of the Bose condensate tunneling through the Gaussian barrier [Eq. (3)]. Start-up kinetic energy per particle of the condensate: $E_0=10$. Gaussian barrier parameters: $V_0=10$ and $\Sigma=1$. Interaction strength: $Na_s/a_z=10$. Comparison among 3D GPE (solid line), 1D NPSE (dotted line), and 1D GPE (dashed line). Length in units of $a_z=(\hbar/m\omega_z)^{1/2}$, density in units of a_z^{-1} , time in units of ω_z^{-1} , and energy in units of $\hbar\omega_z$.

$$V(z) = V_0 e^{-z^2/\Sigma^2}, \quad (13)$$

where V_0 is the height of the potential barrier and Σ its width. The condensate is moved towards the barrier by adding an initial momentum p_0 in the axial direction

$$f(z,0) \rightarrow f(z,0) e^{-ip_0 z/\hbar}. \quad (14)$$

In the case of a noninteracting condensate, i.e., $a_s=0$, the total energy per particle is practically the start-up kinetic-energy $E_0=p_0^2/(2m)$, and the transverse energy $\hbar\omega_\perp$ does not affect the dynamics.

As shown in Fig. 3, where we plot the density profile of the condensate along the symmetry axis at different instants, a fraction of the condensate tunnels the barrier while the rest is reflected. As expected, one sees also the interference between the incident wave function and the reflected wave function. Figure 3 shows that the “exact” axial density profile obtained with the 3D GPE and that of the 1D NPSE are always quite close, also during the impact and tunneling time. These results suggest that 1D NPSE is very adequate also in the description of tunneling phenomena.

The cigar-shaped configuration of the condensate is useful to study topological objects, like bright and dark solitons. By using 1D NPSE one finds out solitonic solutions which generalize what has been previously found with 1D GPE [3,12]. Dark solitons ($a_s>0$) of Bose condensed atoms have been experimentally observed [13], while bright solitons ($a_s<0$) are more elusive due to the collapse of the condensate with a large number of atoms.

Let us first consider bright solitons. Starting from our 1D NPSE, setting $V(z)=0$, scaling z in units of a_\perp and t in units of ω_\perp^{-1} , with the position

$$f(z,t) = \Phi(z-vt) e^{iv(z-vt)} e^{i(v^2/2-\mu)t}, \quad (15)$$

we find

$$\left[\frac{d^2}{d\zeta^2} - 2\gamma \frac{\Phi^2}{\sqrt{1-2\gamma\Phi^2}} + \frac{1}{2} \left(\frac{1}{\sqrt{1-2\gamma\Phi^2}} + \sqrt{1-2\gamma\Phi^2} \right) \right] \Phi = \mu\Phi, \quad (16)$$

where $\zeta=z-vt$ and $\gamma=|a_s|N/a_\perp$. This is a Newtonian second-order differential equation and its constant of motion is given by

$$E = \frac{1}{2} \left(\frac{d\Phi}{d\zeta} \right)^2 + \mu\Phi^2 - \Phi^2 \sqrt{1-2\gamma\Phi^2}. \quad (17)$$

The boundary condition $\Phi \rightarrow 0$ for $\zeta \rightarrow \infty$ implies that $E=0$. Then, by quadratures, one obtains the bright-soliton solution written in implicit form

$$\zeta = \frac{1}{\sqrt{2}} \frac{1}{\sqrt{1-\mu}} \arctan \left[\sqrt{\frac{\sqrt{1-2\gamma\Phi^2}-\mu}{1-\mu}} \right] - \frac{1}{\sqrt{2}} \frac{1}{\sqrt{1+\mu}} \operatorname{arctanh} \left[\sqrt{\frac{\sqrt{1-2\gamma\Phi^2}-\mu}{1+\mu}} \right]. \quad (18)$$

Moreover, by imposing the normalization condition one also finds

$$(1-\mu)^{3/2} - \frac{3}{2}(1-\mu)^{1/2} + \frac{3}{2\sqrt{2}}\gamma = 0. \quad (19)$$

The normalization relates the chemical potential μ to the coupling constant γ , while the velocity v of the bright soliton remains arbitrary. In the weak-coupling limit ($\gamma\Phi^2 \ll 1$), the normalization condition gives $\mu=1-\gamma^2/2$ and the bright-soliton solution reads

$$\Phi(\zeta) = \sqrt{\frac{\gamma}{2}} \operatorname{sech}[\gamma\zeta]. \quad (20)$$

The above solution is the text-book bright soliton of the 1D nonlinear cubic Schrödinger equation (1D GPE). As shown in Fig. 4, for $\sqrt{2}/3 < \gamma < 2/3$ there are two values for the chemical potential μ but we have numerically verified that the lower one corresponds to an unstable solitonic solution. For $\gamma > 2/3$ there are no solitary-wave solutions due to the collapse of the condensate.

In the case of static dark solitons, the boundary conditions are: $\Phi(0)=0$ and $\Phi \rightarrow \Phi_0$ for $z \rightarrow \infty$. Starting from the 1D NPSE the analytical formula of the dark soliton is quite intricate because it involves elliptic integrals. Nevertheless, simple expressions can be found in the weak-coupling and in the strong-coupling limit. In the weak-coupling limits one finds

$$\Phi(z) = \Phi_0 \tanh[\Phi_0 \sqrt{2\tilde{\gamma}}z], \quad (21)$$

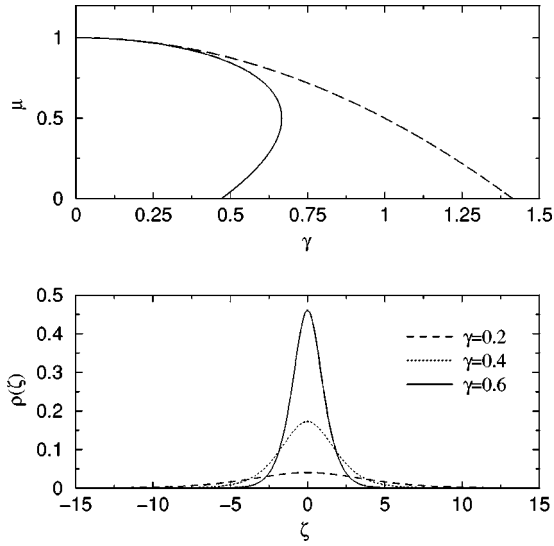


FIG. 4. On the top: chemical potential μ of the bright soliton as a function of the interaction strength $\gamma = |a_s|N/a_\perp$. 1D NPSE (full line) and 1D GPE (dashed line). On the bottom: axial density profile $\rho(\zeta) = \Phi^2(\zeta)$ of the bright soliton of Bose condensed atoms for three values of the interaction strength γ obtained with 1D NPSE.

where $\Phi_0 = \tilde{\gamma}^{1/2}/\sqrt{2}$ and $\tilde{\gamma} = |a_s|\Delta N/a_\perp$, with ΔN the number of missing Bosons due to the hole in the condensate produced by the dark soliton. Equation (20) is the familiar formula of the stationary dark soliton for the 1D nonlinear Schrödinger equation (1D GPE), while in the strong-coupling limit one has

$$|\Phi(z)| = \frac{\Phi_0}{2} (3 \tanh^2[a|z| + b] - 1), \quad (22)$$

where $a = \sqrt{3}\tilde{\gamma}^{1/4}\sqrt{\Phi_0}/2^{3/4}$, $b = \operatorname{arctanh}[1/\sqrt{3}]$, and $\Phi_0 = \tilde{\gamma}^{1/6}/[\sqrt{2}(\sqrt{3}-2/3)^{2/3}]$.

The study of the stability of our solitary-wave solutions is left to a future work. Three-dimensional numerical calculations [14] suggest that Bose condensed dark solitons are stable for sufficiently small numbers of atoms or large transverse confinement. Moreover, a recent experiment [15] has shown that dark solitons, created in a spherical Bose condensate, decay into vortex rings.

III. EFFECTIVE 2D EQUATION

In this section we derive the 2D reduction of the 3D GPE equation by using again a variational approach. In this case we take a trapping potential that is harmonic in the axial direction and generic in the transverse direction: $U(\mathbf{r}) = W(x, y) + \frac{1}{2}m\omega_z^2 z^2$. As trial wave function we take the following:

$$\psi(\mathbf{r}, t) = \phi(x, y, t)f(z, t; \eta(x, y, t)) \quad (23)$$

with

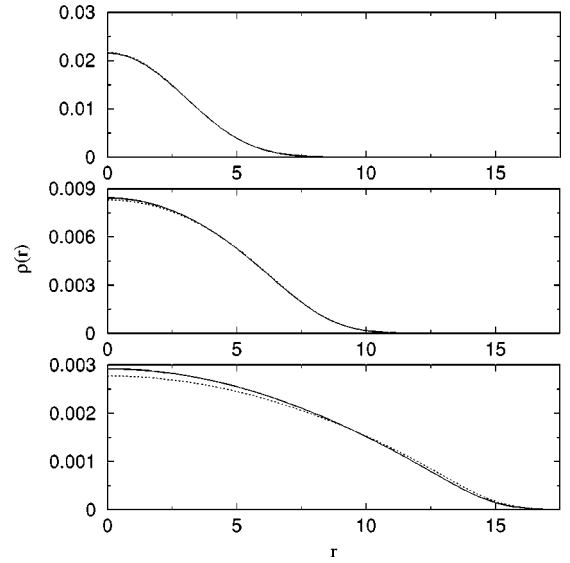


FIG. 5. Radial density profile $\rho(r)$ of the Bose condensate for a disk-shaped trap. Number of Bosons: $N = 10^4$ and trap anisotropy: $\omega_\perp/\omega_z = 1/10$. 3D GPE (solid line) and 2D NPSE (dotted line). From top to bottom: $a_s/a_z = 10^{-4}$, $a_s/a_z = 10^{-3}$, and $a_s/a_z = 10^{-2}$. Length $r = \sqrt{x^2 + y^2}$ in units of a_z and density in units a_z^{-1} .

$$f(z, t; \eta(x, y, t)) = \frac{e^{-z^2/2\eta(x, y, t)^2}}{\pi^{1/4}\eta(x, y, t)^{1/2}}, \quad (24)$$

where $\eta(x, y, t)$ is a variational function that describes the width of the condensate in the axial direction. We assume that the axial wave-function f is slowly varying along the transverse direction with respect to the axial direction, i.e., $\nabla^2 f \approx \partial^2/\partial z^2$. By inserting the trial wave function in Eq. (2) and after spatial integration along the z variable, one finds the following Euler-Lagrange equations:

$$i\hbar \frac{\partial}{\partial t} \phi = \left[-\frac{\hbar^2}{2m} \nabla_\perp^2 + W + gN \frac{\eta^{-1}}{(2\pi)^{1/2}} |\phi|^2 + \left(\frac{\hbar^2}{2m} \eta^{-2} + \frac{m\omega_z^2}{2} \eta^2 \right) \right] \phi, \quad (25)$$

$$\frac{\hbar^2}{2m} \eta^{-3} - \frac{1}{2} m\omega_z^2 \eta + gN \frac{\eta^{-2}}{2(2\pi)^{1/2}} |\phi|^2 = 0. \quad (26)$$

Note that the second Euler-Lagrange equation can be written as $\eta^4 - 2(2\pi)^{1/2} a_z^4 a_s N |\phi|^2 \eta - a_z^4 = 0$, and, contrary to the case of 1D reduction, it does not have an elegant analytical solution but it can be easily solved [16]. We name the 2D nonpolynomial Schrödinger Eq. (25), with the condition (26), 2D NPSE. In Fig. 5 we compare the radial density profile $\rho(r)$ of the Bose condensate obtained by solving 2D NPSE with the exact one obtained by solving the 3D GPE. For simplicity, we use a harmonic trapping potential $W(x, y) = \frac{1}{2}m\omega_\perp^2(x^2 + y^2)$ also in the transverse radial direction. Figure 5 shows that 2D NPSE is quite reliable in describing the ground state of disk-shaped Bose condensate.

For example, the relative error in the calculation of the density at the origin ranges from 0.7 to 5 % by increasing a_s/a_z .

We can analyze the limits of weak and strong interaction of 2D NPSE. In the weakly interacting case one finds $\eta = a_z$ and the equation of motion becomes

$$i\hbar \frac{\partial}{\partial t} \phi = \left[-\frac{\hbar^2}{2m} \nabla_{\perp}^2 + W + \frac{gN}{(2\pi)^{1/2} a_z} |\phi|^2 \right] \phi, \quad (27)$$

where the constant $\hbar \omega_z$ has been omitted because it does not affect the dynamics. This equation is a 2D Gross-Pitaevskii equation. The nonlinear coefficient g'' of this 2D GPE can be thus obtained from the nonlinear coefficient g of the 3D GPE by setting $g'' = g / [(2\pi)^{1/2} a_z]$. Equation (27) describes a disk-shaped Bose condensate in a quasi-2D configuration. In fact, the weakly interacting limit corresponds to a condensate with a chemical potential lower than $\hbar \omega_z$ [8]. In the strongly interacting case one has instead $\eta = \sqrt{2\pi}^{1/3} a_z^{4/3} a_s^{1/3} N^{1/3} |\phi|^{2/3}$, and the resulting nonlinear Schrödinger equation is

$$i\hbar \frac{\partial}{\partial t} \phi = \left[-\frac{\hbar^2}{2m} \nabla_{\perp}^2 + W + \frac{3}{4} \frac{gN^{2/3}}{\pi^{2/3} a_z^{4/3} a_s^{1/3}} |\phi|^{4/3} \right] \phi. \quad (28)$$

Note that in this limit, and in the stationary case, the kinetic term can be neglected (Thomas-Fermi approximation) and one finds the following analytical formula for the transverse density profile:

$$|\phi(x,y)|^2 = \frac{1}{3\sqrt{3}\pi} \frac{1}{(\hbar \omega_z)^{3/2} a_s a_z N} [\mu'' - W(x,y)]^{3/2}, \quad (29)$$

where μ'' is the chemical potential, fixed by the normalization condition. The same dependence is obtained starting from the Thomas-Fermi approximation of the stationary 3D GPE, i.e., neglecting the spatial derivatives in Eq. (1), and

then integrating along the z variable. In this way one finds a formula that differs from the previous one only for the numerical factor which is $\sqrt{2}/(3\pi)$ instead of $1/(3\sqrt{3}\pi)$.

IV. CONCLUSIONS

We have found that the 1D nonpolynomial nonlinear Schrödinger equation we have obtained by using a Gaussian variational ansatz from the 3D Gross-Pitaevskii action functional is quite reliable in describing the ground state and axial collective oscillations of cigar-shaped condensates. We have also tested the accuracy of the nonpolynomial nonlinear equation in the case of a Bose condensate scattering and tunneling on a Gaussian barrier. The agreement with the results of the 3D Gross-Pitaevskii equation is very good for both ground state and the dynamics of the condensate. This equation will be useful for detailed numerical analysis of the *dynamics* of cigar-shaped condensates, particularly when the local density may undergo sudden and large variations. In fact, the accurate mapping we have provided, allows us to maintain a very good spatial resolution with modest computational effort even if the breakdown of the weak interaction condition during time evolution prevents the use of a standard 1D GP equation. This case is often encountered in the study of reflection and tunneling events and in the propagation of solitary waves, which are currently being experimentally investigated. By using the 1D nonpolynomial Schrödinger equation we have obtained analytical formulas for bright and dark solitons which generalize the ones known in the literature for the 1D nonlinear cubic Schrödinger equation. Finally, we have deduced effective 2D equations describing the axial dynamics of disk-shaped condensates. From the 3D Gross-Pitaevskii action functional and using another Gaussian variational ansatz we have derived the effective 2D nonlinear Schrödinger equation, which again has a nonpolynomial structure. This structure simplifies in the weak and strong interacting regime.

-
- [1] E.P. Gross, *Nuovo Cimento* **20**, 454 (1961); L.P. Pitaevskii, *Zh. Éksp. Teor. Fiz.* **40**, 646 (1961); [*Sov. Phys. JETP* **13**, 451 (1961)].
- [2] M. Olshanii, *Phys. Rev. Lett.* **81**, 938 (1998).
- [3] A.D. Jackson, G.M. Kavoulakis, and C.J. Pethick, *Phys. Rev. A* **58**, 2417 (1998).
- [4] M.L. Chiofalo and M.P. Tosi, *Phys. Lett. A* **268**, 406 (2000).
- [5] A.L. Fetter, *Ann. Phys. (N.Y.)* **70**, 67 (1972).
- [6] V.M. Pérez-García, H. Michinel, J.I. Cirac, M. Lewenstein, and P. Zoller, *Phys. Rev. Lett.* **77**, 5320 (1996); *Phys. Rev. A* **56**, 1424 (1997).
- [7] A. Parola, L. Salasnich, and L. Reatto, *Phys. Rev. A* **57**, R3180 (1998).
- [8] A. Görlitz *et al.*, e-print cond-mat/0104549.
- [9] L. Tonks, *Phys. Rev.* **50**, 955 (1936); M. Girardeau, *J. Math. Phys.* **1**, 516 (1960); E.H. Lieb and W. Liniger, *Phys. Rev.* **130**, 1605 (1963); D.S. Petrov, G.V. Shlyapnikov, and J.T.M. Walraven, *Phys. Rev. Lett.* **84**, 2551 (2000).
- [10] E.B. Kolomeisky, T.J. Newman, J.P. Straley, and X. Qi, *Phys. Rev. Lett.* **85**, 1146 (2000).
- [11] E. Cerboneschi, R. Mannella, E. Arimondo, and L. Salasnich, *Phys. Lett. A* **249**, 495 (1998).
- [12] P.O. Fedichev, A.E. Muryshev, and G.V. Shlyapnikov, *Phys. Rev. A* **60**, 3220 (1999); Th. Bush and J.R. Anglin, *Phys. Rev. Lett.* **84**, 2298 (2000).
- [13] S. Burger *et al.*, *Phys. Rev. Lett.* **83**, 5198 (1999); J. Denschlag *et al.*, *Science* **287**, 97 (2000).
- [14] D.L. Feder, M.S. Pindzola, L.A. Collins, B.I. Schneider, and C.W. Clark, *Phys. Rev. A* **62**, 053606 (2000).
- [15] B.P. Anderson *et al.* *Phys. Rev. Lett.* **86**, 2926 (2001).
- [16] Analytical solutions can be found by using the Ferrari-Cardano method for quartic equations, see for instance, V.J. Katz, *A History of Mathematics—An Introduction* (Addison-Wesley, New York, 1998).